2012

Vortex Patterns Beyond Hypergeometric

Andrei Ludu
Embry-Riddle Aeronautical University, ludua@erau.edu

JGSP **26** (2012) 85–103

JOURNAL OF
Geometry and Symmetry
in Physics

VORTEX PATTERNS BEYOND HYPERGEOMETRIC

ANDREI LUDU

Communicated by Boris Konopeltchenko

Abstract. We prove that loop vortices are created by a point-like magnetic dipole in an infinite superconductor space. The geometry of the vortex system is obtained through analytic solutions of the linearized Ginzburg-Landau equation described in terms of Heun functions, generalizing the traditional hypergeometric behavior of such magnetic singularity.

1. Introduction

Three-dimensional superconducting structures allow interesting physical properties such as giant vortices or multi-vortex states, or even (for larger size) a combination of the two states. The traditional approach relies on the Ginzburg-Landau (GL) free-energy minimization procedure, performed on a basis of linear combinations of solutions of the corresponding linearized GL equation [9,21,28]. While finite mesoscopic superconductor samples (size comparable to coherence length ξ, and penetration depth λ) of different geometries, subjected to external uniform magnetic field, have been theoretically investigated [4, 9, 17, 21, 27, 28, 31, 32], there are no exact theoretical models proving that vortex states are possible in unbounded space. In this case the presence of an external applied magnetic field is un-physical (requests infinite energy) and one needs to generate the magnetic field from a localized source. A simple example of this type, which is investigated in this paper, is a microscopic magnetic dipole placed at the origin of an infinite three-dimensional superconducting space. Such types of magnetic field were studied in [25] and it was numerically demonstrated the existence of interconnected vortex loops for spherical or prismatic boundaries. Attempts to solve similar equations in the presence of an electric dipole, have been made [22]. The Coulomb problem for a class of general Natanzon confluent potentials was exactly solved in [16] by reducing the corresponding system to confluent hypergeometric differential equations. More recently in [2], the authors succeed to solve the eigenvalue wave equation for an electron in the field of a molecule with an electric dipole moment by expanding the solutions of a second order Fuchsian differential equation

with regular singularities in a series of Jacobi polynomials with "dipole polynomial" coefficients. However, in all these situations, separation and integration of the Schrödinger equation was possible because the resulting second order ordinary linear differential equations are of Fuchsian type, with maximum three regular singularities. Such equations can be mapped into several types of hypergeometric differential equations.

For the magnetic dipole case the situation becomes more complicated because the order of singularities growths above the hypergeometric range [20, 26, 33]. For example, in the case of a charged particle moving on a sphere under a radial magnetic field and Coulomb force the Schrödinger equation is transformed into a Heun equation. Separation of variables is still possible since the vector potential in this case depends only on one spherical variable θ [23]. Another case of application of Heun equation is presented by the interaction of three particles in a plane, with a perpendicular magnetic field [24]. Here the Schrödinger equations brake into biconfluent Heun's equations because of higher order singularities induced by the Coulombian interaction. Similar problems related to magnetic field (finite-gap potentials, Fokker-Planck, central two-point connection, generalized central potentials up to order $1/r^6$, Hawking radiation, etc.) were approached in literature and usually the resulting leading differential equation for the wave function reduces to one of the Heun's differential equations [10]. An interesting review and study on the use of the Heun's type of differential equations as generalizations of the hypergeometric ones, in relation to supersymmetry, is given in [29], where a two Coulomb-center problem is solved based on a self-adjoint separation of coordinates in prolate spheroidal coordinates.

The paper is organized as follows. In Section 2 we introduce the theoretical formalism and we solve analytically the linearized equation the eigenfunction problem. In Section 3 we obtain solutions for the full nonlinear Ginzburg-Landau problem by minimizing the free energy, and we present surfaces of constant order parameter value in order to identify the multi-vortex structures generated by the magnetic dipole in the mesoscopic superconducting sphere.

2. The Linear Equation

The free-energy in the GL theory is given by the functional [9]

$$F = \int_V \frac{\mathrm{d}v}{V}\left[\frac{1}{2m}|\vec{P}\Psi|^2 + \alpha|\Psi|^2 + \frac{\beta}{2}|\Psi|^4 + \frac{\vec{h}^2}{8\pi}\right] \tag{1}$$

where $\Psi(\vec{r})$ is the order parameter, q, m are the Cooper pairs charge and mass, and $\alpha < 0, \beta > 0$ are the second-order phase transition coefficients. If we investigate the order parameter in a region smaller than the penetrating length λ, yet comparable to the coherence length ξ, we can neglect the contribution to the free-energy of the term responsible by the expulsion of magnetic flux from the superconductor [4, 9, 31]. The singularity of the magnetic field consists in an infinitesimal magnetic dipole of relative strength $\mu = \mu_{\text{magn}}/\mu_0$ placed at the origin and directed along the z axis. The GL equation become

$$\frac{1}{2m}\vec{P}^2\Psi + \alpha\Psi + \beta|\Psi|^2\Psi = 0 \tag{2}$$

where the electromagnetic momentum $\vec{P}$ is given by

$$\overrightarrow{P} = \frac{\hbar}{\mathrm{i}}\overrightarrow{\nabla}(r,\theta,\varphi) - \frac{q\mu}{c}\frac{\sin\theta}{r^2}\overrightarrow{e}_{\varphi}. \tag{3}$$

The linear GL eigenvalue problem associated to equation (2) consists in substituting $|\Psi|^2$ from the last term with a constant denoted $\Lambda > 0$. In dimensionless variables $\Psi \to \sqrt{-\alpha/\beta}\Psi$, $\vec{r} \to \vec{r}/\xi$ with $\xi = \hbar/\sqrt{-2m\alpha}$ the linearized equation becomes

$$\frac{\vec{P}^2}{\hbar^2} = -\left(\overrightarrow{\nabla} - \frac{q\mu}{c}\frac{\sin\theta}{r^2}\overrightarrow{e}_{\varphi}\right)^2\Psi = (1-\Lambda)\Psi \equiv E\Psi \tag{4}$$

where we have the physical condition $E < 1$ requested by the normalization $|\Psi|^2 = 1$. The operator in equation (4) is essentially self-adjoint, [17], so its spectrum is positive, continuous, and unbounded from above by the Leinfelder-Simader, [8], and Miller-Simon theorems [19]). In the following we use dipole coordinates, [30], defined by

$$a = \frac{r}{\sin^2\theta}, \qquad b = \frac{r^2}{\cos\theta}. \tag{5}$$

Usually the dipole coordinates are used in systems controlled by magnetic dipolar terms, where the field lines have strong anisotropy like terrestrial ionosphere, solar corona, magnetostars, toroidal magnetic moments in atomic physics, etc. [11]. The coordinates curves are either double-intersecting loops for a =const., or tangent loops for b =const., Fig.1. The surfaces of coordinates defined by a =const. follow the field lines of the magnetic dipole. In dipole coordinates the electromagnetic momentum has the expression

$$\overrightarrow{P} = \frac{\hbar}{\mathrm{i}}\overrightarrow{\nabla}(a,b,\varphi) - \frac{\chi}{a}\overrightarrow{e}_{\varphi} \tag{6}$$

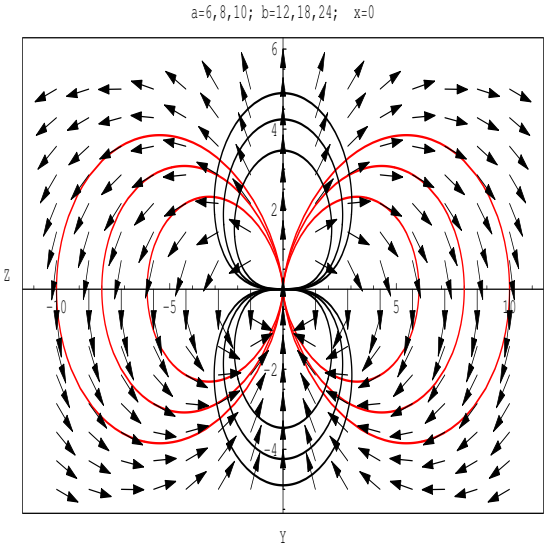

Figure 1. Curves of orthogonal coordinates of constant $a = 6, 8, 10$ (red loops), and constant $b = 12, 8, 24$ (black loops) in the $x = 0$ plane. The dipole is directed along z axis with arrows describing the magnetic field.

where we denoted $\chi = q\mu/c$. In the following we investigate only solutions with good orbital quantum number L (vorticity), i.e., $\Psi = \Phi(a, b)\mathrm{e}^{\mathrm{i}\varphi L}$. By introducing equation (6) in equation (4), we obtain a partial differential equation in (a, b)

$$\left(\frac{a}{r}\right)^3\left(1+3\frac{r^4}{b^2}\right)\left(\frac{\mathrm{d}^2\Phi}{\mathrm{d}a^2}+\frac{4}{1+\frac{3r^4}{b^2}}\frac{1}{a}\frac{\mathrm{d}\Phi}{\mathrm{d}a}\right)+\left(1+3\frac{r^4}{b^2}\right)\frac{b^2}{r^6}\frac{\mathrm{d}}{\mathrm{d}b}\left(b^2\frac{\mathrm{d}\Phi}{\mathrm{d}b}\right)$$
$$-\frac{a}{r^3}\left(L-\frac{\chi}{a}\right)^2\Phi+E\Phi=0 \quad (7)$$

where the real number $E < 1$ is a free parameter.

In order to obtain a separation of the dipole variables (a, b) we investigate solutions of equation (7) in the range $a >> b$, which describes points close to the z-axis. The reason for this hypothesis is that the order parameter has a much stronger $a-$dependence than the one on b. Consequently, $|\Psi|$ =const. are similar to surfaces a =const. Under this hypothesis equation (7) reduces to the form

$$\frac{\partial^2\Phi}{\partial a^2}+\frac{4}{a}\frac{\partial\Phi}{\partial a}+\frac{b^2}{a^6}\frac{\partial}{\partial b}\left(b^2\frac{\partial\Phi}{\partial b}\right)-\frac{1}{a^2}\left(L-\frac{\chi}{a}\right)^2\Phi+E\Phi=0 \quad (8)$$

and we can factorize the b-dependence from the a-dependence

$$\Phi(a,b)=Q(a)\left(\mathrm{e}^{-\frac{c_1}{b}}+C_0\mathrm{e}^{\frac{c_2}{b}}\right) \quad (9)$$

where $c_{1,2}$ are constants of integration. The resulting equation for $Q(a)$ is

$$a^6\frac{\mathrm{d}^2Q}{\mathrm{d}a^2}+4a^5\frac{\mathrm{d}Q}{\mathrm{d}a}+(c^2-\chi^2a^2+2L\chi a^3-L^2a^4+Ea^6)Q=0. \tag{10}$$

Equation (10) is an ordinary differential equation of order two with meromorphic coefficients. It has two irregular singularities of rank 2, $a=0,\infty$, [12], and consequently there are no convergent solutions in terms of Frobenius series.

In the following, we study the solutions with $c_1=0$ because we expect these subspace of solutions to fulfill the hypothesis above about the $|\Psi|^2$ iso-surfaces laying along the dipole surface coordinates a =constant. For these solutions equation (10) becomes

$$\frac{\mathrm{d}^2Q}{\mathrm{d}a^2}+\frac{4}{a}\frac{\mathrm{d}Q}{\mathrm{d}a}+\left(-\frac{\chi^2}{a^4}+\frac{2L\chi}{a^3}-\frac{L^2}{a^2}+E\right)Q=0. \tag{11}$$

Equation (11), i.e., the "dipole" equation, has two asymptotic solutions. In the far range limit $a\to\infty$, by neglecting higher order terms in $1/a$, we have

$$Q^{\infty}(a)=a^{-\frac{3}{2}}\left(C_1J_{\sqrt{L^2+\frac{9}{4}}}(\sqrt{E}a)+C_2Y_{\sqrt{L^2+\frac{9}{4}}}(\sqrt{E}a)\right) \tag{12}$$

where J,Y are the Bessel functions of the first and the second kind, respectively, and $C_{1,2}$ arbitrary constants of integration. In the close-range limit $a\to 0$, by neglecting lower orders in $1/a$, we have

$$Q^{0}(a)=\mathrm{e}^{-\frac{\chi}{a}}\left[C_1M\left(2-L,4;\frac{2\chi}{a}\right)+C_2U\left(2-L,4;\frac{2\chi}{a}\right)\right] \tag{13}$$

where M and U are the Kummer and Tricomi confluent hypergeometric functions, respectively.

In the following, by using the transformations

$$Q(\tilde{z})=\tilde{z}^{\xi_0}\mathrm{e}^{\xi_1\tilde{z}-\frac{\xi_{-1}}{\tilde{z}}}y(\tilde{z}),\qquad a\to\tilde{z}=a\lambda^{1/4}/(\sqrt{\mathrm{i}}\chi) \tag{14}$$

we map the dipole equation equation (10) into a symmetric canonical double-confluent Heun equation in $y(\tilde{z})$ [6, 13–15, 26].

$$\tilde{D}^2y+\alpha\left(\tilde{z}+\frac{1}{\tilde{z}}\right)\tilde{D}y+\left[\left(\beta_1+\frac{1}{2}\right)\alpha\tilde{z}+\left(\frac{\alpha^2}{2}-\gamma\right)+\left(\beta_{-1}-\frac{1}{2}\right)\frac{\alpha}{\tilde{z}}\right]y=0 \tag{15}$$

where $\lambda=E/\chi^2$, $\tilde{D}=\tilde{z}(\mathrm{d}/\mathrm{d}\tilde{z})$, and

$$\alpha=\pm 2\mathrm{i}\sqrt{\mathrm{i}}\lambda^{1/4},\qquad \beta_1=0,\qquad \beta_{-1}=\mp L,\qquad \gamma=L^2+9/4. \tag{16}$$

Working with the symmetrical canonical form provides a recursion relation for the series coefficients of the analytic solution in only three terms. Also, this form depends on less parameters, and provides trivial relations between asymptotical solutions at zero and infinity (central connection problem) [6, 15].

Since we study the no-boundary problem we construct the solutions of equation (15) based on the asymptotic behavior for $\tilde{z} \to \infty$. The continuation of this solution towards the origin is performed through the central connection relations between asymptotic solutions, such that the behavior at zero of the fundamental solution fulfills the regularity condition for Ψ in zero.

In order to obtain a first fundamental solution for DCHE we use the asymptotic construction of the solution of equation (15) following the receipt in [26]. The functions

$$\begin{aligned} y_{\infty 1}(\alpha,\beta,\gamma;\tilde{z}) &= \Theta(\alpha,\beta,\gamma;\tilde{z}) \\ y_{\infty 2}(\alpha,\beta,\gamma;\tilde{z}) &= \mathrm{i}\mathrm{e}^{-\mathrm{i}\pi\beta_1}\mathrm{e}^{-\alpha\tilde{z}}\Theta(\mathrm{e}^{\mathrm{i}\pi/2}\alpha,\beta_{-1},-\beta_1,\gamma;\mathrm{e}^{\mathrm{i}\pi/2}\tilde{z}) \end{aligned} \tag{17}$$

where the holomorphic function Θ is defined as

$$\Theta(\alpha,\beta,\gamma;\tilde{z}) = (\alpha\tilde{z})^{-\beta_1-\frac{1}{2}}\sum_{n=0}^{\infty}\Theta_n(\alpha\tilde{z})^{-n} \tag{18}$$

in the range on arg $(\alpha\tilde{z}) \in (-\pi/2, 5\pi/2)$, with coefficients uniquely given by the three-term recursion relation

$$\Theta_n^{\pm} = \frac{1}{n}\left[\left(\frac{\alpha^2}{2}-\gamma+\left(n+\beta_1-\frac{1}{2}\right)^2+\right)\Theta_{n-1}^{\pm}-\alpha^2(n+\beta_1-\beta_{-1}-1)\Theta_{n-2}^{\pm}\right] \tag{19}$$

with $n \in \mathbb{N}$, $\Theta_{-1}^{\pm} = 0, \Theta_0^{\pm} = 1$, constitute a fundamental solution for the symmetric canonical DCHE, equation (15). The signs $\pm$ represent the choice for one of the two solutions for the reduced parameters α, β_{-1} in equation (16). The second solution $y_{\infty 2}$ is generated from the first one by application of the group operator T_1, and it is linear independent from the first, as one can check through the Wronskian calculation.

The solution in equation (18) provides a unique asymptotic behavior for $\tilde{z} \to \infty$ in the forms

$$\begin{aligned} y_{\infty 1}(\tilde{z}) &= (\alpha\tilde{z})^{-\beta_1-\frac{1}{2}}\left[1+O\left(\frac{1}{\tilde{z}}\right)\right], \qquad \arg(\alpha\tilde{z}) \in \left(-\frac{\pi}{2},\frac{5\pi}{2}\right) \\ y_{\infty 2}(\tilde{z}) &= \mathrm{e}^{-\alpha\tilde{z}}(\alpha\tilde{z})^{\beta_1-\frac{1}{2}}\left[1+O\left(\frac{1}{\tilde{z}}\right)\right], \qquad \arg(\alpha\tilde{z}) \in \left(-\frac{3\pi}{2},\frac{3\pi}{2}\right). \end{aligned} \tag{20}$$

The parameters $\alpha, \beta_{\pm 1}$ control the behavior of the solution at $\tilde{z} \to \infty$, while χ controls the behavior in zero. Depending on the sign of the eigenvalue $\lambda < 1/\chi^2$ there are possible several combinations of signs in equations (17) which fulfil the request for the argument of the expression $\alpha\tilde{z}$ to belong in the prescribed sectors, equations (20), assuring holomorphic solutions on $a \in (0, \infty)$. It is important to take into account the allowed combinations, because in the real variables $A(a)$ holomorphism assures analyticity of the order parameter, which is essential for the self-adjoint property of the generic equation equation (4). For example, if $\lambda < 0$ there are only five admissible combinations of signs among the 32 possible combinations in $\alpha = \pm 2(\sqrt{-\mathrm{i}})_{1,2}(\lambda^{1/4})_{1,\ldots,4}$, and in $(\sqrt{\mathrm{i}})_{1,2}$ as part of the substitution $a \to \tilde{z}$. For $0 < \lambda < 1/\chi^2$ there are more favorable cases, and only five forbidden combinations of signs. We do not table here all these combinations, because we show in the following that all these reduce to one single viable solution. By performing back

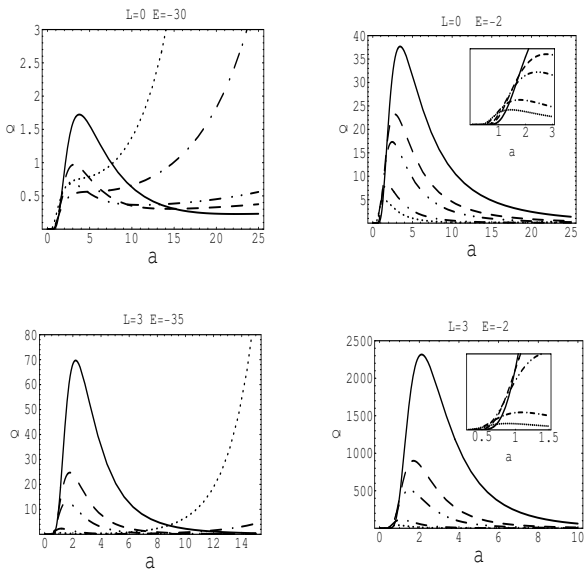

Figure 2. Examples of solutions, equations (21) and (23), for $L = 0$ ($E = -30, -2$), $L = 3$ ($E = -35, -2$). We present the case of four different values of relative dipole strength, $\chi = 1, 3, 6, 8$. They are plotted from gray to black, correspondingly, the stronger dipole being associated to the darkest line.

the substitutions in the independent and dependent variable, we obtain the physical solutions for the a dependent part of the order parameter. Namely, from $y_{\infty 1}$ we

obtain the solution

$$A_{\infty 1}(a)=\left(\frac{\chi}{a}\right)^{\frac{3}{2}}\exp\left[\pm_1 \mathrm{i}\frac{E^{1/2}a}{\chi^2}\pm_2\frac{\chi}{a}\right]\left(\pm_3 2\mathrm{i}\frac{E^{1/2}a}{\chi^2}\right)^{-\frac{1}{2}} \times\sum_{n=0}^{\infty}\Theta_n^{\pm_3}\left(\pm_3 2\mathrm{i}\frac{E^{1/2}a}{\chi^2}\right)^n \quad (21)$$

and recursion relation for the series coefficients

$$\Theta_n^{\pm}=\frac{1}{n}\left[\left(n^2-n-L^2-2-2\mathrm{i}\frac{E^{1/2}}{\chi}\right)\Theta_{n-1}^{\pm} +4\mathrm{i}(n\pm L-1)\frac{E^{1/2}}{\chi}\Theta_{n-2}^{\pm}\right]. \quad (22)$$

From $y_{\infty 2}$ we have respectively

$$A_{\infty 2}(a)=\mathrm{i}\left(\frac{\chi}{a}\right)^{\frac{3}{2}}\exp\left[\mp_1 \mathrm{i}\frac{E^{1/2}a}{\chi^2}\pm_2\frac{\chi}{a}\right]\left(\mp_3 2\mathrm{i}\frac{E^{1/2}a}{\chi^2}\right)^{\pm_3-\frac{1}{2}} \times\sum_{n=0}^{\infty}\Omega_n^{\pm_3}\left(\mp_3 2\mathrm{i}\frac{E^{1/2}a}{\chi^2}\right)^n \quad (23)$$

with recursion relation

$$\Omega_n^{\pm}=\frac{1}{n}\left[\left(n^2-n-2\pm L\mp 2nL+2\mathrm{i}\frac{E^{1/2}}{\chi}\right)\Omega_{n-1}^{\pm} -4\mathrm{i}(n\mp L-1)\frac{E^{1/2}}{\chi}\Omega_{n-2}^{\pm}\right]. \quad (24)$$

In these equations the symbols $\pm_{\mathrm{i}}$ mean that we can choose the sign plus or minus in an arbitrary, independent way for different j values. Also, the $\pm$ having the same subscript should be synchronized in all expressions. We present in Fig. 2 some examples of the solutions in equations (21) and (23). We notice that in general solutions intersect for different values of the parameters. For large negative energies the solutions become divergent at infinity, which means that the convergence radius of the series was exceeded, or from the physical point of view, such energies are unlikely to be realized. Higher values for angular momentum shrink the wave functions towards the origin, and left it oscillating with smaller amplitude towards the surface of the sample.

2.1. Qualitative Analysis of the Linear Solutions

Equations (21)-(24) represent the most general set of exact solutions of the linearized dipole equation. These solutions depend parametrically on χ, L and E. It is useful to mention that for positive energies, $0 < E < 1$, the solutions are bounded on $[0, \infty]$ and are oscillating functions. Their asymptotic value towards $a \to \infty$ is a linear combination of Bessel functions of real argument and imaginary order. In the range of negative energies, $E < 0$, the solutions have real exponential decay towards infinity, asymptotically described by Bessel functions of imaginary argument and real order. In this range the solutions are still bounded, do not oscillate. However, under some constrains, they can be truncated to polynomials.

Such special truncations, very useful for analytic and numeric calculation, are possible for $E < 0$, and only for the series coefficients that have negative sign in front of L, in their second term on the right hand side, of the recursion relations. For each L value there is one unique value of the energy which provides the truncation of the series into a quasi-polynomial (the series reduces to a polynomial, but the exponentials and powers in front of it, equations (21) and (23), still remain. The algorithm is simple. We arrange for any L that the coefficient of the second term on the right hand side in the expression of Θ_n^- (Ω_n^+) to cancel, that is $n-L-1=0$, which fixes $n = L + 1$. Next we solve the equation $\Theta_L^- = 0$ ($\Omega_L^+ = 0$) for E. These two conditions guarantee the cancelation of all terms with $n > L$, so the series reduces to a polynomial. For example if we choose $L = 1$ we have the solution

$$A_{\infty 1}(a) = \frac{\chi^2}{\sqrt{3}a^2} \mathrm{e}^{-\frac{3a}{2\chi}-\frac{\chi}{a}}, \qquad E = -\frac{9\chi^2}{4}. \tag{25}$$

Another example for $L = 3$ reads

$$A_{\infty 1}(a) = \frac{\chi^2}{\sqrt{w_1}a^2} \mathrm{e}^{-\frac{w_1 a}{2\chi}-\frac{\chi}{a}} \left[1 + \Theta_1^- \frac{\chi}{w_1 a} + \Theta_2^- \left(\frac{\chi}{w_1 a}\right)^2\right] \tag{26}$$

with

$$E = -\frac{\chi^2 w_1^2}{4}$$

where $\Theta_{1,2}^-$ are obtained from equation (22). Example of quasi-polynomial solutions are given in Fig. 3. Quasi-polynomial can be constructed for negative energies an d only odd angular momenta. For $A_{\infty 2}$ the majority of solutions are with $E > 0$ so they do not provide quasi-polynomials.

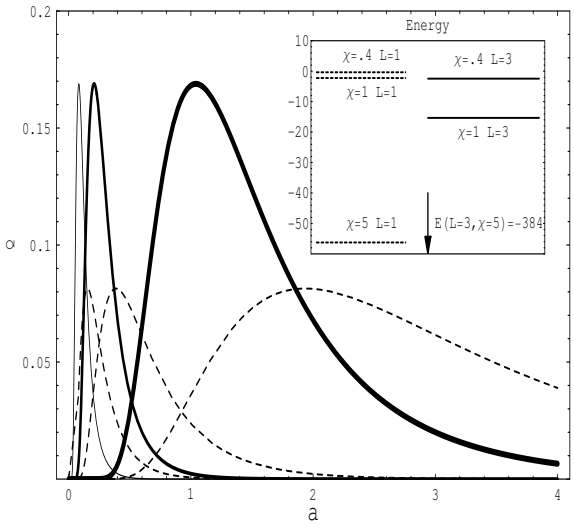

Figure 3. Example of linear order parameter quasi-polynomial solutions, equations (25) and (26), for $L = 1$ (dotted line wave functions), $L = 3$ (solid line) for three different values of the dipole strengths ($\chi = 0.4, 1, 5$). We represent the increasing of strength by the increasing of thickness of plotted lines. The corresponding energies for the cases where the series truncate are plotted in the smaller window. For small dipole strength values the levels at different angular moments are almost degenerated.

The regular behavior of the solutions in the $a \to \infty$ limit is guaranteed by the asymptotic construction in equations (17), through the general theory of the Heun's differential equation. For any value of the energy and angular momentum, these solutions approach zero for $a \to \infty$, since, from the asymptotic expressions of $y_{\infty 1,2}$ the leading term to infinity is

$$a^{-2} \mathrm{e}^{-\frac{\mathrm{i}\sqrt{E}a}{\chi^2}}.$$

Consequently, no matter of the sign of E the exponential has either negative real coefficient, or imaginary coefficient, so the $a \to \infty$ limit of the magnitude of the solutions is zero in any situations. Towards ∞ both solutions approach zero by dumped oscillations because, for very large value of a, the dipole equation reduces to a modified Bessel equation. Hence, the solution in equations (17) approaches asymptotically at infinity the product between $a^{-3/2}$ and a combination of Bessel functions, equation (12). For example, it is enough to use just the first four terms in equation (18) to note this asymptotical behavior, see Fig. 4. This behavior can be

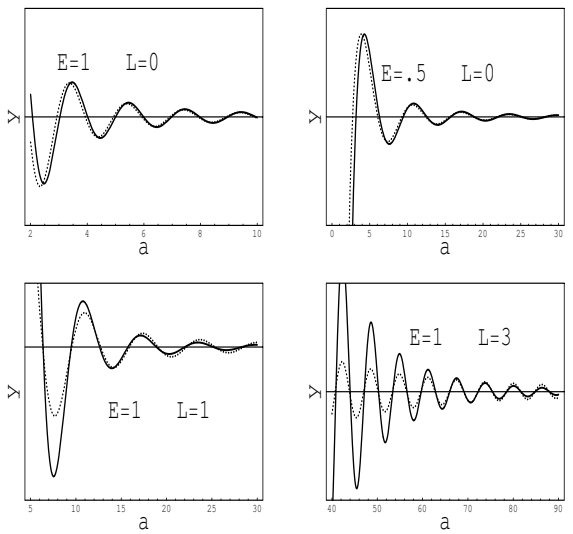

Figure 4. Asymptotic behavior at ∞ of the analytic solution of the dipole equation. The real part of the sum of the first four terms in the series solutions, equation (21), (continuous line) is compared with the Bessel function times exponential and power solutions, equation (27), of the asymptotic form of the dipole equation (dotted line) for large values of a. We compared for $L = 0$ for two different energies, and for $L = 1, 3$ for the maximum admissible value of the energy E, ($\chi = 1$).

proved by comparing the asymptotic behavior of solution in equation (12) towards infinity.

In order to have an evaluation of the asymptotic behavior of solutions towards infinity, more accurate than the one in equation (20), we need to use the canonical form equation (15). So, by neglecting terms in $1/z$ in this equation we reduce it to a Bessel asymptotic form with exact solutions for $a \to \infty$

$$A_\infty \to A^{\text{Bessel}} = \left(\frac{\chi}{a}\right)^{\frac{3}{2}} \mathrm{e}^{-\frac{\chi}{a}} \left[C_1 J_{\sqrt{\frac{9}{4}+L^2+\frac{2\mathrm{i}E^{1/2}}{\chi}}} \left(\frac{E^{1/2}a}{\chi^2}\right) + C_2 Y_{\sqrt{\frac{9}{4}+L^2+\frac{2\mathrm{i}E^{1/2}}{\chi}}} \left(\frac{E^{1/2}a}{\chi^2}\right) \right] \quad (27)$$

where J, Y are the Bessel functions of first and second kind, respectively.

3. Vortex Patterns

The solution for the nonlinear dipole equation $\Psi^{NL}(a,b,\varphi)$ can be constructed as a linear combination of exact analytic solutions of the linear problem, equations (21) and (23). We introduce the following notation for the linear solutions basis

$$\Psi_{L,E}(a,\varphi) = Q_{\infty 1}(L,E;a)\mathrm{e}^{\mathrm{i}L\varphi}. \tag{28}$$

We search nonlinear solutions of the form

$$\Psi^{NL}(a,\varphi) = \sum_{L=0}^{L_{\max}} \int_0^{E_{\max}(L)} C_{L,E}\Psi_{L,E}(a,\varphi)\mathrm{d}E \tag{29}$$

with $C_{L,E}$ parameters to be determined. In order to generate physical solutions for the full nonlinear GL problem, the expression equation (29) is plugged in the Gibbs free energy expression equation (1) and this integral is minimized in the space of parameters $C_{L,E}$.

In the following we prove that it is enough to investigate order parameters built by only two linear solutions (see similar approaches in [27, 28]). This limitation does not reduce the generality of the treatment and has enough structure to put into evidence the existence of multi-vortex patterns. We have

$$\Psi^{NL} = C_1 Q_{\infty 1,L_1,E_1}(a)\mathrm{e}^{\mathrm{i}L_1\varphi} + C_2 Q_{\infty 1,L_2,E_2}(a)\mathrm{e}^{\mathrm{i}L_2\varphi} \tag{30}$$

with $C_{1,2}$ free real coefficients. We transform the Gibbs free energy functional, written in the above chosen dimensionless units ($F \to F/F_0 = \beta F/\alpha^2$) and in the approximation of sufficient small samples, in the form

$$F = 2\int_V \frac{\mathrm{d}v}{V}\left(\frac{1}{\hbar^2}\Psi^{NL*}|\vec{P}|^2\Psi^{NL} - |\Psi^{NL}|^2 + \frac{1}{2}|\Psi^{NL}|^4\right). \tag{31}$$

Following the standard numerical procedure for minimization, [4, 9, 21, 27, 28, 31, 32], we plug the test function equation (30) in the functional equation (31) and look for minima. With the notations

$$\begin{aligned} D_i &= \int \frac{\mathrm{d}v}{V}(\Psi^{NL})^4_{\infty 1,L_i,E_i}, \qquad S_i = \int \frac{\mathrm{d}v}{V}(\Psi^{NL})^2_{\infty 1,L_i,E_i} \\ D &= \int \frac{\mathrm{d}v}{V}(\Psi^{NL})^2_{\infty 1,L_1,E_1}(\Psi^{NL})^2_{\infty 1,L_2,E_2} \end{aligned} \tag{32}$$

where the integrals are evaluated all over $\mathbb{R}^3$. We calculate the free energy functional equation (31) for the functions in equation (30). The the integration over

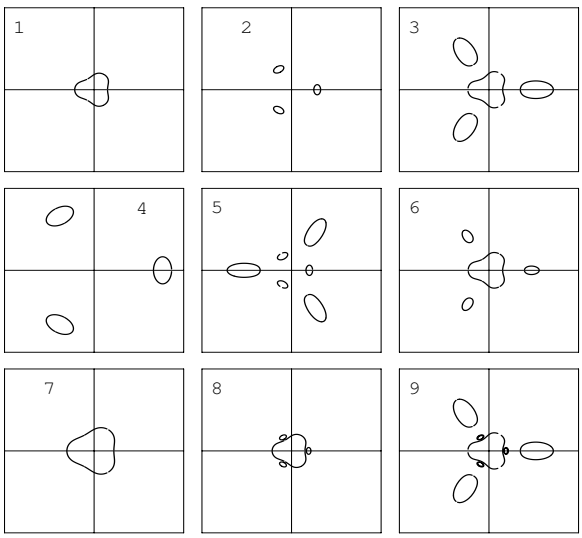

Figure 5. Contour plots of the intersection of surfaces $|\Psi^{NL}| = 0.9$ with the plane $z = 0.8R$. We choose $a = 100, L_1 = 0, L_2 = 3, E_1 = 0, E_2 = 1$. When the strength is increased, $\chi = 0.6, 0.8, \ldots, 2.2$, we plot different frames, from $1, \ldots, 9$, respectively. Three vortex loop structure is formed from an initially connected domain around the origin. For higher dipole strength three symmetric loops (frames 2-6) are generated and grow together with the core. In frame 7 they tend to brake into open vortices and become unstable. For higher values of χ, frames 8-9, three new loops are formed again, and so on.

b produces a multiplicative constant in front of each symbol from equations (32). Since the space of free parameters for the F minimization is two-dimensional, we can use the Hessian matrix method to find the minima of F. The resulting expression for F is much simplified because we use for test functions the analytical solutions of the linearized problem. By introduction equation (30) in equation (31), and by using equation (32) and the orthonormality properties of $Q_{\infty 1}$, we obtain, [4, 7], the following values for the two coefficients that minimize the free energy

$$C_1 = \pm\sqrt{\frac{-(E_1-1)D_2S_1 + 2(E_2-1)DS_2}{D_1D_2 - 4D^2}}$$
$$C_2 = \pm\sqrt{\frac{-(E_2-1)D_1S_2 + 2(E_1-1)DS_1}{D_1D_2 - 4D^2}}. \tag{33}$$

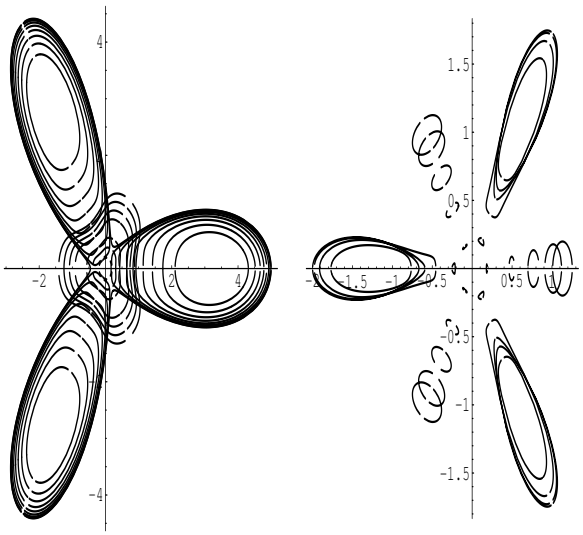

Figure 6. Same three vortex loop dynamics from Fig. 5, except we overlap frames 1-4 and 6-8 in the left graphics, and overlap frames 5,9 in the right graphics.

For these value of the coefficients the Gibbs free energy equation (31) becomes

$$F[C_{1,2}] = [-(E_1-1)^2 D_2 S_1^2 - (E_2-1)^2 D_1 S_2^2 \\ + 4(E_1-1)^2(E_2-1)^2 D S_1 S_2] \times (D_1 D_2 - 4D^2)^{-1}. \quad (34)$$

Consequently, when we restrict to combinations of two linear eigenfunctions, stable nonlinear solutions of the GL problem are provided by equation (30) with the coefficients from equations (33), while the physical energy of the system is given by equation (34). It results that for every set of parameters $E_{1,2}, L_{1,2}$, and χ we can find a nonlinear solution $\Psi^{NL}(a,\varphi)$ which minimizes the free energy.

In order to describe multi-vortex states of vorticity L we need to prove the existence of stable solutions of the type equation (30) with the property that it exists a number $a_v \in (0,\infty)$ such that the equation $|\Psi^{NL}(a_v,\varphi)| = 0$ has n distinct solutions for $\varphi \in [0,2\pi)$, denoted $\varphi_j, j = 1,2,\ldots,n$. Indeed, since the solutions Φ are analytic, there are always neighborhoods of a_v on which $|\Psi^{NL}|$ is arbitrary small for the corresponding roots φ_j. The surfaces described by the values of a in these neighborhoods are isoplots of multi-vortex structure, and the centerlines of the vortices are the curves obtained by the intersections of the $a = a_v$ and $\varphi = \varphi_j$ surfaces. For example, if we choose $L_1 = 0$, and $L_2 = 3$ we expect to find a structure with $L_2 - L_1 = 3$ disjoint vortices.

We can prove the following final result: for any χ, and for any pair $L_{1,2}$, there is always a pair $E_{1,2}$ such that the nonlinear solution of the GL equation in the form of equation (30), with coefficients given by equations (33) for the set $L_{1,2}, E_{1,2}$ provides a confined multi-vortex state of vorticity $n = |L_2 - L_1|$. The stability of such states is described by the relative values of the corresponding free energy, equation (34). The proof consists in showing that we can always find a number $a_v \in (0, \infty)$ such that the equation in φ

$$-\frac{C_1 Q_{\infty 1, L_1, E_1}(a)}{C_2 Q_{\infty 1, L_2, E_2}(a)}\bigg|_{a=a_v} = \mathrm{e}^{\mathrm{i}(L_2 - L_1)\varphi}$$

has n solutions $\varphi_j \in [0, 2\pi)$, $j = 1, 2, \ldots, n$. The sufficient condition is to show that we can find $k_{1,2}$ such that

$$\left|\frac{C_1 Q_{\infty 1, L_1, E_1}(a_v)}{C_2 Q_{\infty 1, L_2, E_2}(a_v)}\right| \arg(C_1 Q_{\infty 1, L_1, E_1}(a_v)) \geq 1 \tag{35}$$

for $a_v < \infty$. It results that it always exists some a_v for any $\chi, L_{1,2}$ such that this condition is fulfilled for at least on set of $E_{1,2}$ because the functions $Q_{\infty 1, L_i, E_i}(a)$ have asymptotical Bessel type of oscillating behavior towards ∞. Consequently, the numerator $Q_{\infty 1, L_1, E_1}(a)$ is arbitrary small at least at a point where the denominator is different from zero (linear independent solutions with Bessel function asymptotic behavior have isolated zeros, and different zeros for different orders).

The value a_v is chose to be the one which provides the minimum value of F among all minima for different E_2. The angular positions of the vortices central lines are given by

$$\varphi_j = \left[\arccos\left(\frac{1 + \left(\frac{|C_2 Q_{\infty 1, L_2, E_2}(a_v)|}{|C_1 Q_{\infty 1, L_1, E_1}(a_v)|}\right)^2}{2\frac{|C_2 Q_{\infty 1, L_2, E_2}(a_v)|}{|C_1 Q_{\infty 1, L_1, E_1}(a_v)|}}\right)\right.$$
$$\left. + \arg(C_1 Q_{\infty 1, L_1, E_1}(a_v)) - \arg(C_1 Q_{\infty 1, L_2, E_2}(a_v)) \pm j\pi\right] \cdot (L_1 - L_2)^{-1}$$

with $j = 1, 2, \ldots, |L_1 - L_2|$, and $|\cdot|$ and $\arg$ being the modulus and the argument of the complex numbers. To visualize a simple example of a multi-vortex state, we choose a large value for $a_v = 100$, and we choose $L_1 = 0, k_1 = 0$, and $L_2 = 0, \ldots, 4$.

In Fig. 5 we present a dynamical situation, namely the generation of a compact structure of three vortex loops. While the dipole strength is increased from 0.6 to 2.2 a ferromagnetic central domain is formed and three vortex loops are generated

out of this core. The loops grow in size together with the core, and this can be noticed in frames 2-6 of Fig. 5 initially the horizontal cross section at $z = 0.8R$ intersect the tops of the loops (frames 2,4), then the cross section intersects the middle of loops (each loop cut twice by this pane, frames 5,9), and then the plane intersects the core, too (frames 3,6,8). In Fig. 6 we plot the same three vortex loops dynamics, except we overlap frames 1-4, 6-8 from Fig. 5 in the left graphics, and we overlap frames 5,9 in the right graphics of Fig. 6. In this representation one can see that the vortices are indeed separated from the core, forming a loop structure. Finally, we plot in Fig. 7 the Gibbs free energy of the configurations presented in Fig. 5 and Fig. 6 which proves the stability of the obtained loop vortices.

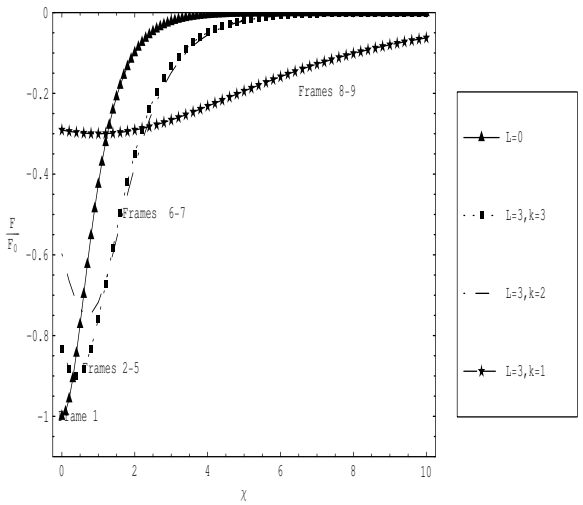

Figure 7. Free energy plot versus the strength of the magnetic dipole for $L_1 = 0, L_2 = 3$. One can notice phase transitions between different geometries of the vortices towards minimum of the free energy.

4. Conclusions

We investigate the existence of confined vortex loops in a superconducting infinite space, where the magnetic field is generated by a point-like magnetic dipole placed at the origin. We use a Ginzburg-Landau model in the approximation of weak magnetic field. The Euler-Lagrange PDE equations emerging from this free energy functional reduce to a magnetic Schrödinger equation. Exact solutions are obtained in dipole coordinates a, b, φ. In order to integrate the linearized dipole

equation we confine our calculations in regions closer to the poles of the sphere. Also, we consider that the gradient of the order parameter function is mainly directed radial and orthogonal to the magnetic dipole field lines. Consequently, the order parameter is almost constant along these lines, and the coordinate surfaces a =const. describe the vortex surfaces. We found that the exact solution of the dipole equation obtained through this procedure in the form of Heun functions are enough to prove the occurrence of spontaneous vortex phase, where vortices interconnect at the origin. We study the analytic solutions of the linearized dipole equation by mapping it into a double confluent Heun equation. We build linear combinations of two solutions of the linearized dipole equation and look for confined vortex structures. Among these combination of linear solutions we choose those that minimize the free energy functional and we consider them as solutions of the full nonlinear problem. We prove that multi-vortex states are possible even without the presence of an external applied field, and they are generally characterized by confined vortex loops. We determine the symmetries of the confined phase starting from solutions of the linearized Ginzburg-Landau, and we also compare these analytic results with previous numerical results [9, 25].

Acknowledgements

This research was partially supported through the Condensed Matter Theory Group of Antwerp University, Belgium. The author is indebted to Mauro Doria for the idea of and motivation in writing this article, to Andre Ronveaux for the interesting discussions on the Heun functions, and to Francois Peeters and Milorad Milosevic for help, support during my sabbatical year and their valuable comments.

References

[1] Abramowitz M. and Stegun I., *Handbook of Mathematical Functions*, Natl. Bureau of Standards, Washington, DC 1964.

[2] Alhaidari A. and Bahlouli H., *Electron in the Field of a Molecule with an Electric Dipole Moment*, Phys. Rev. Lett. **100** (2008) 110401-4.

[3] Arfken G., *Mathematical Methods in Physics*, Orlando, Academic Press 1970.

[4] Baelus B., Sun D. and Peeters F., *Vortex Structures in Mesoscopic Superconducting Spheres*, Phys. Rev. B **75** (2007) 174523-11.

[5] Boyce W. and di Prima R., *Elementary Differential Equations and Boundary Value Problems*, John Wiley & Sons, New York 1977.

[6] Bühring W., *The Double Confluent Heun Equation*: *Characteristic Exponent and Connection Formulae*, Meth. Appl. Anal. **1** (1994) 348-370.

[7] Chen Y., *Vortex Matter in a Mesoscopic Superconducting Cone*, PhD Thesis, Universiteit Antwerpen, Antwerpen 2007.

[8] Cycon H., Froese R., Kirsch W. and Simon B., *Schrödinger Operators*, Springer, Berlin 1987.

[9] Doria M., de Romaguera A. and Peeters F., *Effect of the Boundary Condition on the Vortex Patterns in Mesoscopic Three-dimensional Superconductors*: *Disk and Sphere*, Phys. Rev. B **75** (2007) 064505-7.

[10] Debosscher A., *Unification of One-dimensional Fokker-Planck Equations Beyond Hypergeometrics*: *Factorizer Solution Method and Eigenvalue Schemes*, Phys. Rev. E. **57** (1998) 252-275.

[11] Fatkullin M. and Sitnov Yu., *A Dipolar Coordinate System and Some of its Characteristics*, Geomagn. Aeronomy **12** (1972) 293-295.

[12] Hille E., *Lectures on Ordinary Differential Equations in the Complex Domain*, Willey, New York 1976.

[13] Hounkonnou M., Ronveaux A. and Sodoga K., *Factorization of Some Confluent Heun's Differential Equations*, Appl. Math. Comp. **189** (2007) 816-820.

[14] Kazakov A., *The Central Two-point Connection Problem for the Reduced Confluent Heun Equation*, J. Phys. A: Math. & Gen. **39** (2006) 2339-2348.

[15] Lay W., Bay K. and Slavyanov S., *Asymptotic and Numeric Study of Eigenvalues of the Double Confluent Heun Equation*, J. Phys. A: Math. & Gen. **31** (1998) 8521-8532.

[16] Lévai G. and Williams B., *The Generalized Coulomb Problem*: *An Exactly Solvable Model*, J. Phys. A: Math. & Gen. **26** (1993) 3301-3306.

[17] Ludu A., van Deunn J., Milosevic M., Cuyt A. and Peeters F., *Analytic Treatment of Vortex States in Cylindrical Superconductors in Applied Axial Magnetic Field*, J. Math. Phys. **51** (2010) 082903-29.

[18] Magnus W. and Winkler S., *Hill's Equation*, Interscience, New York 1966.

[19] Miller K. and Simon B., *Quantum Magnetic Hamiltonians with Remarkable Spectral Properties*, Phys. Rev. Lett. **44** (1980) 1706-1707.

[20] Moon P. and Spencer D., *Field Theory Handbook*, Springer, Berlin 1971.

[21] Palacios J., *Metastability and Paramagnetism in Superconducting Mesoscopic Disks*, Phys. Rev. Lett. **84** (2000) 1796-1799.

[22] Picca D., *The Dipolar Potential*, J. Phys. A: Math. & Gen. **15** (1982) 2801-2808.

[23] Ralko A. and Truong T., *Heun Functions and the Energy Spectrum of a Charged Particle on a Sphere Under a Magnetic Field and Coulomb Force*, J. Phys. A: Math. & Gen. **35** (2002) 9573-9584.

[24] Ralko A. and Truong T., *Behaviour of Three Charged Particles on a Plane Under Perpendicular Magnetic Field*, J. Phys. A: Math. & Gen. **35** (2002) 9671-9684.

[25] de Romaguera A., Doria M. and Peeters F., *Transverse Magnetization and Torque in Asymmetrical Mesoscopic Superconductors*, Phys. Rev. B **76** (2007) 020505-4.

[26] Ronveaux A., *Heun's Differential Equations*, Oxford University Press, Oxford 1995.

[27] Schweigert V. and Peeters F., *Phase Transitions in Thin Mesoscopic Superconducting Disks*, Phys. Rev. B **57** (1998) 13817-13832.

[28] Schweigert V., Peeters F. and Deo P., *Vortex Phase Diagram for Mesoscopic Superconducting Disks*, Phys. Rev. Lett. **81** (1998) 2783-2786.

[29] Stahlhofen A., *Susy, Gauss, Heun and Physics*: *A Magic Square?*, J. Phys. A: Math. & Gen. **37** (2004) 10129-10138.

[30] Swisdak M., *Notes on the Dipole Coordinate System*, arXiv:physics/0606044v1 (2006) 1-6.

[31] Xu B., Milosevic M. and Peeters F., *Magnetic Properties of Vortex States in Spherical Superconductors*, Phys. Rev. B **77** (2008) 144509-9.

[32] Zha G.-Q., Zhou S.-P., Zhu B.-H., Shi Y.-M. and Zhao H.-W., *Superconducting Phase Transitions in Thin Mesoscopic Rings With Enhanced Surface Superconductivity*, Phys. Rev. B **74** (2006) 024527-9.

[33] Zwillinger D., *Handbook of Differential Equations*, Academic Press, San Diego 1998.

Andrei Ludu
Department of Mathematics
Embry-Riddle Aeronautical University
32114 Daytona Beach, USA
E-mail address: ludua@erau.edu